Histol Histopathol (1996) 11: 103-110

Histology and Histopathology

Fine structure of the acinar and duct cell components in the parotid and submandibular salivary glands of the rat: a TEM, SEM, and HRSEM study

I. Watanabe[1], H. Seguchi[2], T. Okada[2], T. Kobayashi[2], Q.S. Jin[2] and X.D. Jiang[2]

[1]Department of Anatomy, Institute of Biomedical Sciences, University of Sao Paulo, Brazil and

[2]Department of Anatomy and Cell Biology, Kochi Medical School, Okoh-cho, Nankoku, Kochi, Japan

Summary. Parenchymal and stromal components of the rat parotid and submandibular glands were examined by conventional and high resolution scanning electron microscopy (HRSEM). Freeze-fractured specimens were subjected to HCl and NaOH extraction procedures to better differentiate connective tissue and cellular components. In addition, the internal three-dimensional morphology of the secretory acinar cells and duct cells was revealed by maceration with a dilute osmium tetroxide solution to selectively remove some of the cytoplasmic components. SEM and HRSEM examination of the HCl-treated samples of both glands revealed a fine filamentous network immediately surrounding each acinus. Coarser bundles of collagen that linked neighboring acini were also observed. NaOH-extracted samples selectively removed the cellular components and showed more clearly the three-dimensional structure of the connective-tissue stroma. A dense-collagenous network surrounded each lobule while more internal regions consisted of a honeycomb-like pattern of evacuated spaces previously occupied by secretory acini. These spaces were smoothened in appearance and often interconnected. Apically-located secretory granules and profiles of the rough endoplasmic reticulum and Golgi apparatus in perinuclear regions were encountered in the acinar and duct cells of macerated samples by HRSEM. In addition, a phenylephrine-induced experimental condition performed in some rats resulted in a significant increase in secretory granule size and density of the serous cells.

Key words: Parotid gland, Submandibular gland, Ultrastructure, HRSEM, Phenylephrine

Offprint requests to: Dr. I. Watanabe, Instituto de Ciencias Biomedicas, Universitaria de São Paulo, Cidade Universitaria, CEP 05508-900, Sao Paulo, SP, Brazil

Introduction

The parotid and submandibular glands are compound tubuloacinar exocrine glands that secrete a high proportion of the saliva into the oral cavity. Ultrastructural studies of the parotid gland have been performed in many different mammalian species including the spider monkey (Leeson, 1969), pig (Boshell and Wilborn, 1978), mongolian gerbil (Ichikawa and Ichikawa, 1975), rat (Hand, 1972), human (Riva and Riva-Testa, 1973; Riva et al., 1974, 1988, 1993a), and rabbit (Watanabe et al., 1989). Common findings of these studies indicate that the parotid gland is composed almost exclusively of serous-secreting cells, whereas studies of the submandibular gland (Leeson and Jacob, 1959; Tamarin and Sreebny, 1965; Tandler and Poulsen, 1976; Brocco and Tamarin, 1979; Pinkstaff, 1980; Espinal et al., 1983; Hazen-Martin and Simson, 1986; Watanabe et al., 1992a,b) have revealed that, in many species, the secretory acini may contain cells of the either the serous type or the mucous type or a combination of the two. Moreover, rodent submandibular glands have been shown to contain specialized secretory cells known as granulated convoluted tubule cells which are found in a segment of the excretory duct lying between intercalated and striated ductal regions (Tamarin and Sreebny, 1965; Caramia, 1966; Hazen-Martin and Simon, 1986).

Many of these studies have been restricted to the use of TEM and, therefore, have made it difficult to appreciate the three-dimensional organization of these complex secretory structures. Recent advancements in HRSEM techniques and instrumentation have made it possible to observe details of cellular structure at magnifications approaching those of TEM (Hollenberg and Lea, 1988). This study was undertaken with the aim of elucidating the three-dimensional ultrastructure of the parotid and submandibular glands of the rat using the aldehyde-osmium-DMSO-osmium-DMSO-osmium (A-

O-D-O) procedure (Tanaka, 1989) and pH-dependent selective-extraction procedures (Evan et al., 1976; Ohtani, 1987). In addition, the effects of phenylephrine, an α-adrenergic agonist that has been shown to be an effective stimulator for release of stored materials from salivary secretory cells (Wallace and Partlow, 1976; Simson et al., 1978, 1979; Vreugdenhil et al., 1980; Hazen-Martin and Simson, 1986) was studied to determine the ultrastructural changes that occur in the cellular components of the acinar and secretory duct cells.

Materials and methods

Eight adult male Sprague Dawley rats weighing approximately 200 gr were used in this study. The control group animals were anesthetized by intraperitoneal injection of sodium pentobarbital and were sacrificed by ventricular perfusion with a modified Karnovsky fixative containing 0.5% glutaraldehyde and 0.5% paraformaldehyde in 0.067M sodium cacodylate buffer (pH 7.2).

In the experimental group, the animals were injected intraperitoneally with 0.5 mg/animal phenylephrine (Sigma Chemical Co., St. Louis, MO, USA) in 0.85% physiological saline. Five minutes following secretagogue, the animals were sacrificed via left ventricular perfusion of the Karnovsky fixative solution. The parotid and submandibular salivary glands were, subsequently, dissected out, cut into small pieces, and fixed for an additional 3 hrs at 4 ºC in the same fixative solution.

For transmission electron microscopy, both control and experimental group specimens were rinsed in phosphate buffer (pH 7.2) and postfixed in 1% osmium tetroxide diluted in 0.1M sodium cacodylate buffer (pH 7.2). The tissues were dehydrated through a graded series of ethanols, followed by propylene oxide, and them embedded in Spurr's resin (Spurr, 1969). Thin sections were obtained using a Reichert Ultracut-E (C. Reichert AG, Vienna, Austria) and were stained with methanolic uranyl acetate and lead citrate. The sections were examined under a JEOL 1200 EX transmission electron microscope (JEOL Co., Tokyo, Japan).

For scanning electron microscopy, small pieces of both the control and experimental tissues were fixed in a buffered glutaraldehyde solution for 3 hrs at 4 ºC. They were then rinsed in distilled water for 30 minutes, postfixed in 2% osmium tetroxide and treated with the A-O-D-O method as described by Tanaka (1989). The tissues were immersed in 12.5%, 25% and 50% of DMSO and fractured in a 50% DMSO solution using an Eiko TF-2 apparatus cooled with liquid nitrogen. The fractured specimens were thawed in 50% DMSO, rinsed in distilled water, and postfixed in 2% osmium tetroxide. Additionally, some of the specimens were macerated with a dilute osmium tetroxide solution (0.1%) for 48, 60, and 72 hrs at 20 ºC. Afterwards, they were rinsed in distilled water for at least 3 hrs, postfixed in 2% osmium tetroxide and immersed in 2% tannic acid aqueous solution for 1 hour at room temperature (Murakami, 1974). After being rinsed well in distilled water, the specimens were postfixed with 2% osmium tetroxide solution, washed with distilled water and dehydrated through a graded series of ethanols. They were then immersed in isoamyl acetate solution and critical-point dried with a Hitachi CPD-2 (Hitachi Co., Tokyo, Japan) using liquid CO_2, and coated with platinum-palladium in a Hitachi Ion-Coater 1036. The samples were examined in a Hitachi H-700 SEM, and a Hitachi S-900 high resolution scanning electron microscope.

Specimens were also treated with NaOH or HCl-collagenase solutions to selectively extract cellular and extracellular components, respectively. For scanning electron microscopy, the tissues were fixed by ventricular perfusion with a modified Karnovsky fixative containing 2.5% glutaraldehyde and 2% paraformaldehyde in 0.1M sodium cacodylate buffer (pH 7.2). Specimens were freeze-fractured as previously described and were then treated with a modified method of Evan et al. (1976) that utilized a 3N HCl solution at 4 ºC for several days. Some tissues were also immersed in a 10% NaOH solution for 3 to 7 days at room temperature according to the technique described by Ohtani (1987). Samples were rinsed in distilled water and postfixed in 1% osmium tetroxide in 0.1M sodium cacodylate buffer, dehydrated in a graded series of ethanols, and critical-point dried in a Hitachi CPD-2 using liquid CO_2. They were then mounted on stubs, coated with platinum-palladium in a Hitachi 1036 Ion-Sputter, and examined with a Hitachi S-450 scanning electron microscope.

Results

Freeze-fractured surfaces of the parotid and submandibular salivary glands processed with the A-O-D-O method displayed several lobules which contained a high density of secretory acini and exhibited profiles of secretory and excretory ducts (Fig. 1a). The external surfaces of the acini were clearly observed in the HCl-treated specimens and were characterized by a delicate three-dimensional network of connective-tissue fibers surrounding each acinus (Fig. 1b). Additionally, coarser bundles of collagen fibers traversing the interacinar spaces and linking neighboring acini were also observed. At high magnification, the external surfaces of the acinar secretory cells contained small-diameter connective tissue fibrils that were intimately associated and sometimes embedded within the basement membrane of the cells (Fig. 1c).

NaOH-treated samples observed under the SEM revealed a honeycomb-like network of dense connective tissue stroma devoid of secretory cells (Fig. 2a,b). The hollowed areas, formerly occupied by the secretory acinar cells, displayed interconnections and their inner surfaces were smooth in appearance (Fig. 2b). Each lobule was surrounded by a dense interwoven network of

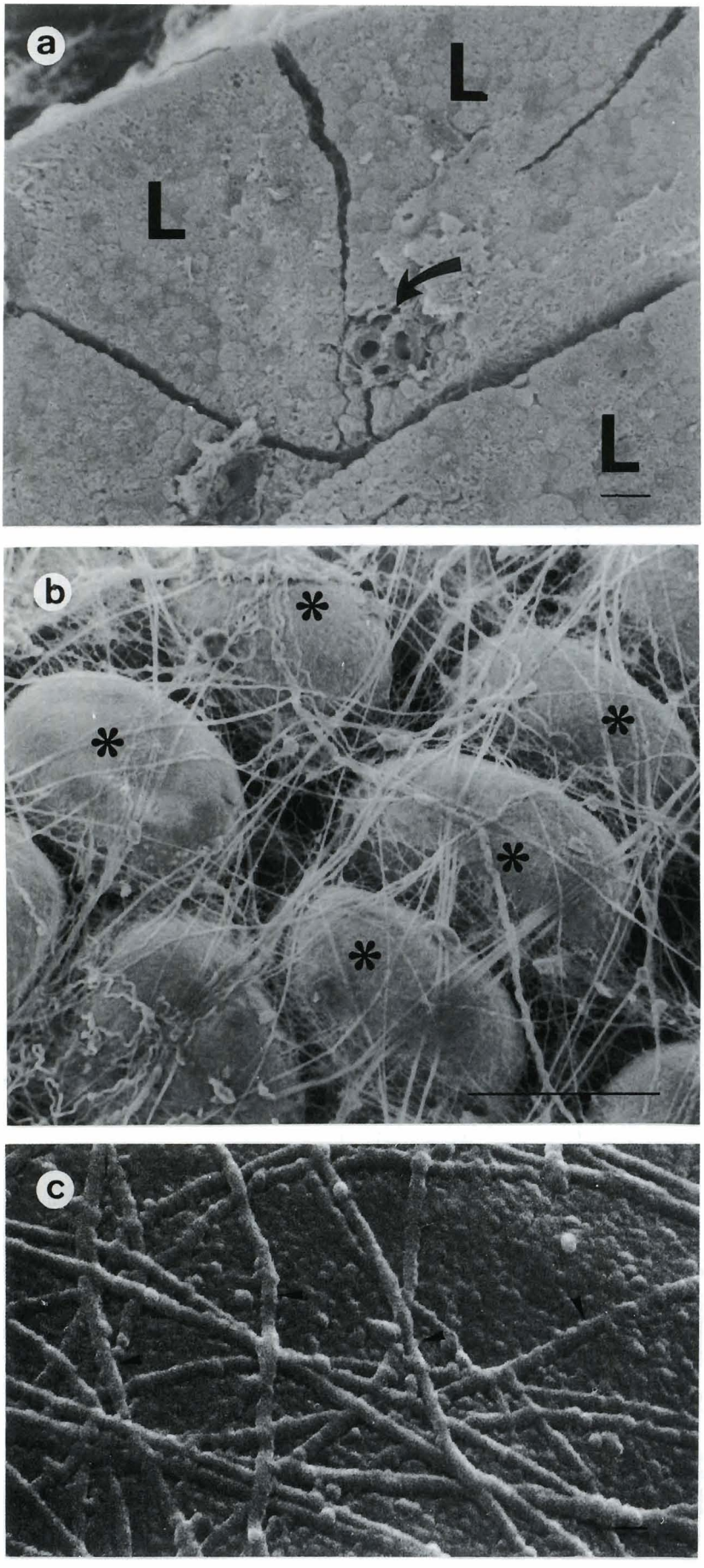

Fig. 1. Freeze-fractured surface of the rat parotid gland following treated with 3N HCl and viewed by SEM at low **(a)**, medium **(b)**, and high magnifications **(c)**. Several lobules (L) of the gland and excretory ducts (curved arrow) embedded in the connective-tissue septa can be observed in a. A delicate three-dimensional supporting connective-tissue network is observed in b with bundles of collagen fibrils spanning the acinar (*) formations. At high magnification (c), the surface of the acinar formations contain a fine network of collagen fibrils (arrow-heads) intimately associated with their surfaces. a) x 160, Bar: 50 µm; b) x 600, Bar: 50 µm; c) x 50,000, Bar: 0.1 µm.

collagen fibers that appeared to be continuous with the interacinar connective-tissue stroma (Fig. 2b). Additionally, the larger excretory ducts contained a thickened connective tissue sleeve which separated the ducts from the acini (Fig. 2c).

In the A-O-D-O treated specimens, the secretory acinar cells exhibited basally-located nuclei and a relatively homogeneous diameter population of apical and supranuclear secretory granules embedded within their cytoplasm (Fig. 3a). Moreover, in the submandibular gland, adjacent mucous-secreting cells were observed and were characterized by a vacuolated cytoplasm and basally-condensed nuclei (Fig.3a). At the apical surfaces of the secretory cells, small acinar canaliculi measuring 1.0 to 1.4 µm in diameter were encountered.

In rats injected with phenylephrine, a higher density and a more heterogeneous collection of secretory granules were seen in the apical regions of the serous cells (Fig. 4a). In TEM sections, these granules varied in electron density and closely abutted each other, and, in some cases, were seen fusing with neighboring granules. A highly-developed Golgi network surrounded these granules and, in basal regions, a dilated and vesiculated rough endoplasmic reticulum could be seen. HRSEM images of the phenylephrine-stimulated serous cells

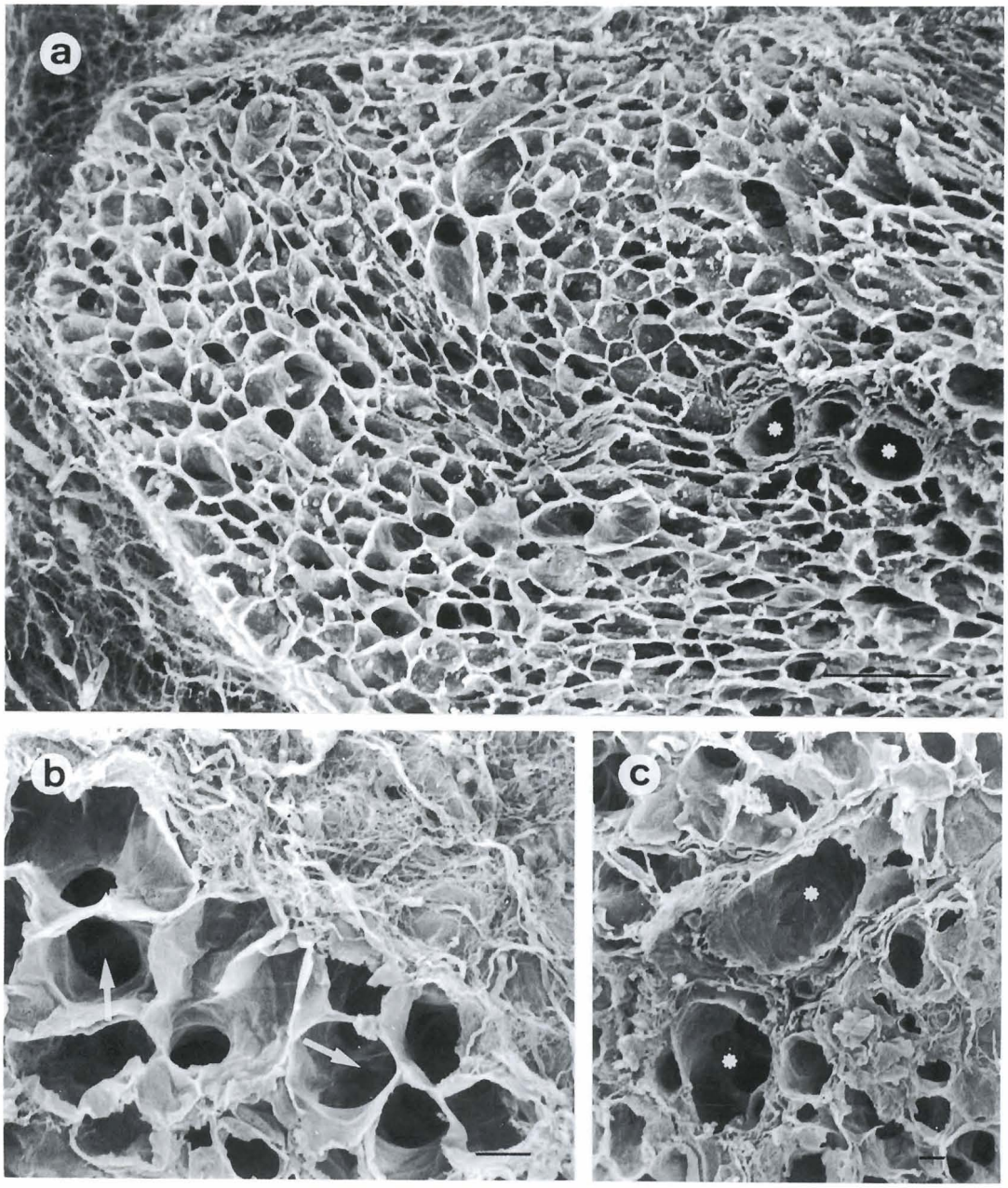

Fig. 2. NaOH-treated parotid gland. At low magnification **(a)**, a honeycomb-like network of connective-tissue stroma is observed. A peripheral portion of the lobule **(b)** and a region containing excretory ducts **(c)** are seen at higher magnifications. Acinar spaces (small arrows) and excretory ducts (*) are indicated. a) x 360, Bar: 50 µm; b) x 750, Bar: 10 µm; c) x 450, Bar: 10 µm.

Fig. 3. Low **(a)** and high **(b)** magnification HRSEM views of a rat submandibular gland macerated for 48 hrs in dilute osmium tetroxide. Several secretory granules (arrowheads) can be seen in the apical and supranuclear regions of the serous cells. Note an adjacent mucous-secreting cell (*) and the lumen of a salivary caniliculus (large arrow). The granules in the apical cytoplasm of the serous cell are seen at higher magnification in b. a) x 9.000. Bar: 1 µm: b) x 36.000. Bar: 0.1 µm.

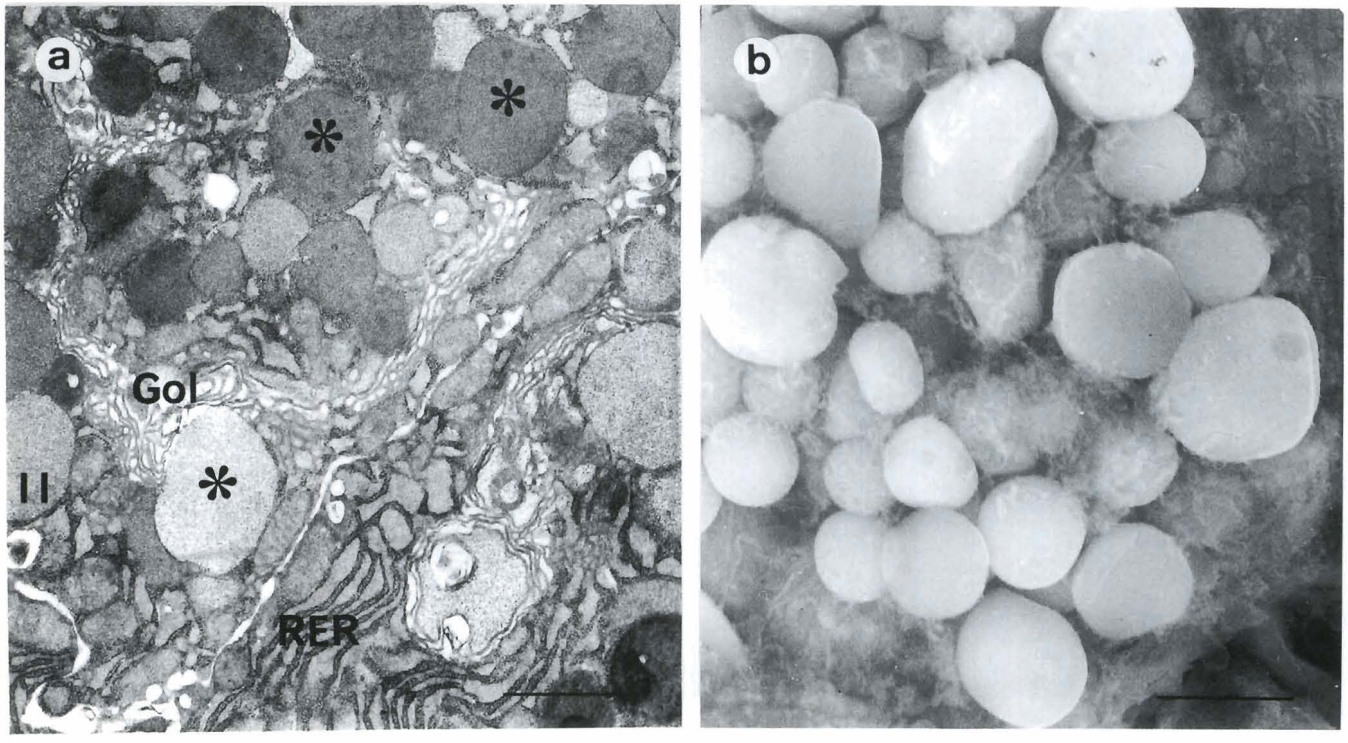

Fig. 4. Phenylephrine-stimulated serous cells of the parotid gland viewed by TEM **(a)** and by HRSEM **(b)**. A dense population of heterogeneously-stained secretory granules (*) is seen near the apical portions of the serous cell in a. Note the developed rough endoplasmic reticulum (RER) and Golgi apparatus (Gol). When viewed by HRSEM (b), many spherical and ellipsoid granules of various sizes can be seen in the apical regions. a) x 18,000, Bar: 1 µm: b) x 17,500, Bar: 1 µm.

were characterized by a tightly-packed collection of spherical to ellipsoid granules in their apical regions with an inconspicuous intervening amorphous substance between them (Fig. 4b).

Granular convoluted tubules were characterized by the presence of truncated pyramidal to columnar cells that contained basally-located nuclei and which possessed a highly-infolded plasmalemma with numerous longitudinally-oriented mitochondria (Fig. 5a). The apical regions exhibited similarly-sized

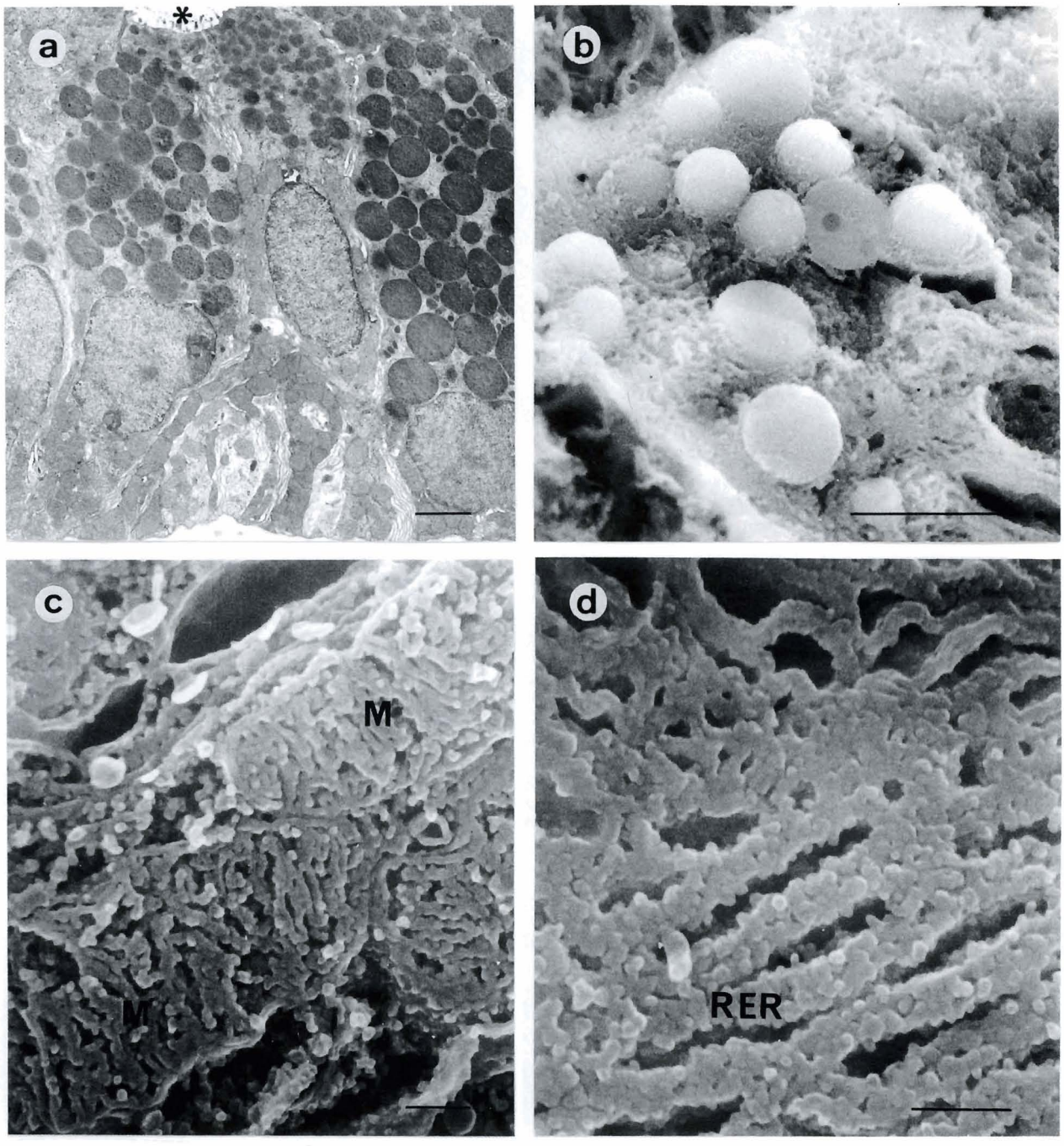

Fig. 5. Striated duct cells observed by TEM **(a)** and HRSEM **(b, c, d)**. The TEM image (a) reveals a number of columnar-shaped striated duct cells with their characteristic basally-located mitochondria and nuclei. Note the dense accumulation of apically-located secretory granules in their cytoplasm and a portion of the secretory duct above (*). The three-dimensional features of the secretory granules are seen in b. A tightly-packed array of mitochondrial cristae can be seen in several fractured mitochondria (M) at the basal regions (c). The rough endoplasmic reticulum (RER) of a secretory duct cell is observed in d. a) x 8,600, Bar: 1 µm; b) x 27,000, Bar: 1 µm; c) x 100,000, Bar: 0.1 µm; d) x 160,000, Bar: 0.1 µm.

granules to those seen in the serous acinar cells (Fig. 5a,b). High-magnification HRSEM images revealed a dense internal cristae network in the fractured mitochondria of basal regions (Fig. 5c). In addition, a ribosome-studded network of rough endoplasmic reticulum was also observed in the basal and perinuclear areas of the secretory duct cells and the serous acinar cells.

Discussion

Our results demonstrate that the HCl-extraction method is a useful technique for revealing external surface morphology of the salivary gland acini and their constituent cells. The specimens prepared by this method displayed a partially-extracted stroma which permitted fine structural observation of the stromal-parenchymal relationship in salivary glands. Images obtained by HRSEM revealed a delicate three-dimensional network of connective-tissue fibrils that appeared to link adjacent secretory acini. An intimate relationship of the fibrils with the basement membranes of the secretory cells was also noted.

Treatment of specimens with the 10% NaOH solution revealed the three-dimensional organization of the connective-tissue stroma of the salivary glands. This method appeared to completely digest the cellular components of the secretory acini and ducts leaving behind a honeycomb-like network of connective tissue. Each lobule was enveloped by a thickened layer of three-dimensionally arranged collagen-fiber bundles which appeared to form a well-defined capsule around the lobules. In addition, the HRSEM data revealed a sleeve-like arrangement of collagen fibrils occupying the interstitial compartment where nerve fibers and capillaries are present.

HRSEM observations made it possible to demonstrate the three-dimensional organization of the cytoplasmic structures of the secretory cells. This method of observation has been utilized with success in several other tissues and cell types (Tanaka, 1981, 1989; Hanaki et al., 1985; Hollenberg and Lea, 1988, 1989; Iwashita and Naguro, 1990; Watanabe et al., 1992a,b; Riva et al., 1993b). Moreover, the maceration technique using dilute osmium tetroxide (Tanaka, 1981) enables a more detailed visualization of intracellular components. The biochemical action of dilute osmium tetroxide is believed to produce an initial gelation and solubilization of cytoplasmic proteins while preserving lipid-containing and membrane-bounded structures (Porter and Kallman, 1953; Lea and Hollenberg, 1989).

The data in the present study showed that the rough endoplasmic reticulum of the acinar and secretory duct cells exhibited a multilamellar structure formed by numerous ribosome-studded flattened cisterna in perinuclear regions. The lumen of the RER also appeared dilated following administration of phenylephrine indicating an increase in activity. The morphology of the mitochondria were clearly noted in three-dimensional images and were shown to possess a compact network of tubular and tubulovesicular cristae. The shape of mitochondrial cristae in different cell types has been controversial for many years, partly due to the limitations of the two-dimensional images obtained by TEM. The presence of tubular cristae in mitochondria of cells from several cell types have been described at both the TEM and HRSEM levels (Wheatly, 1968; Tanaka, 1981; Hanaki et al., 1985; Lea and Hollenberg, 1989) and have been shown to be particularly abundant in adrenal cortical cells and liver hepatocytes. Evidence from HRSEM images in this study suggest that the cristae arrangement is similar in the granulated duct cells of the submandibular gland and may be suggestive of relatively high levels of metabolic activity and possibly steroid synthesis. The function of the cells in the granulated convoluted tubules is still not fully understood, but it has been postulated to be multifaceted due to the presence of numerous basal mitochondria and a relative abundance secretory granules. Moreover, the apically-located granules may have several actions since many different proteins have been described in their secretory granules including amylase, nerve growth factor, renin and esteroproteases (Pasquini et al., 1974; Gresik et al., 1978; Hazen-Martin, 1983).

In summary, a complete appreciation of the ultrastructure of the salivary glands can be achieved only through analysis with a variety of methodologies. In this study, the application of SEM and HRSEM has provided a novel approach for visualization of the stromal and parenchymal components of the parotid and submandibular glands from a three-dimensional perspective. It is hoped that a more complete understanding of the intricate ultrastructural makeup of the salivary glands will contribute to a better understanding of their complex functions.

Acknowledgements. We gratefully acknowledge the assistance of Mr. Patrick Nahirney in the preparation and review of the manuscript. This work was supported by a grant from the Japanese International Cooperation Agency (JICA), 1993.

References

Boshell J.L. and Wilborn W.H. (1978). Histology and ultrastructure of the pig parotid gland. Am. J. Anat. 152, 447-466.

Brocco S.L. and Tamarin A. (1979). The topography of rat submandibular gland parenchyma as observed with SEM. Anat. Rec. 194, 445-460.

Caramia F. (1966). Ultrastructure of mouse submaxillary gland. I. Sexual differences. J. Ultrastruct. Res. 16, 505-523.

Espinal E.G., Ubios A.M. and Cabrini R.L. (1983). Freeze-fracture surface of salivary glands of rat observed by scanning electron microscopy. Acta Anat. 117, 15-20.

Evan A.P., Dail W.G., Dammrose D. and Palmer C. (1976). Scanning electron microscopy of cell surfaces following removal of extracellular material. Anat. Rec. 185, 433-446.

Gresik E., Michelakis A., Barka T. and Ross T. (1978). Immunocyto-

chemical localization of renin in the submandibular gland of the mouse. J. Histochem. Cytochem. 26, 855-861.

Hanaki M., Tanaka K. and Kahsima Y. (1985). Scanning electron microscopic study on mitochondrial cristae in the rat adrenal cortex. J. Electron Microsc. 34, 373-380.

Hand A.R. (1972). The effects of acute starvation on parotid acinar cells. Ultrastructural and cytochemical observations on ad libitum-fed and starved rats. Am. J. Anat. 135, 71-92.

Hazen-Martin D.J. (1983). The effect of secretagogue stimulation on the granular tubule segment of the male mouse submandibular gland: and ultrastructural and immunocytochemical study. Anat. Rec. 205, 78-79A.

Hazen-Martin D.J. and Simson J.A.V. (1986). Ultrastructure of the secretory response of male mouse submandibular gland granular tubules. Anat. Rec. 214, 253-265.

Hollenberg M.J. and Lea P.J. (1988). High resolution scanning electron microscopy of the retinal pigment epithelium and Bruch's layer. Invest. Ophthalmol. Vis. Sci. 29, 1380-1389.

Hollenberg M.J. and Lea P.J. (1989). Advantages of visualization of organelle structure by high resolution scanning electron microscopy. Scanning 11, 157-168.

Ichikawa M. and Ichikawa A. (1975). The fine structure of the parotid gland of the Mongolian Gerbil, *Meriones Meridianus*. Arch. Histol. Jpn. 38, 1-16.

Iwashita K. and Naguro T. (1990). Intracellular structure of the olfactory epithelial cells observed by scanning electron microscopy. Yonago Acta Med. 33, 175-194.

Lea P.J. and Hollenberg M.J. (1989). Mitochondrial structure revealed by high resolution scanning electron microscopy. Am. J. Anat. 184, 245-257.

Leeson C.R. (1969). The fine structure of the parotid gland of the spider monkey. Acta Anat. 72, 133-147.

Leeson C.R. and Jacob F. (1959). An electron microscopic study of the rat submaxillary gland during its post-natal development and in the adult. J. Anat. 93, 287-295.

Ohtani O. (1987). Three-dimensional organization of the connective tissue fibers of the human pancreas: a scanning electron microscopic study of NaOH treated tissues. Arch. Histol. Jpn. 50, 557-566.

Pasquini F., Petris A., Sbaraglia G., Scopelliti R., Cenci G. and Frati L. (1974). Biological activities in the granules isolated from the mouse submaxillary gland. Exp. Cell Res. 86, 233-236.

Pinkstaff C.A. (1980). The cytology of salivary glands. Int. Rev. Cytol. 63, 141-249.

Porter K.R. and Kallman F. (1953). The properties and effects of osmium tetroxide as a tissue fixative with special reference to its use for electron microscopy. Exp. Cell Res. 4, 127-141.

Riva A. and Riva-Testa F. (1973). Fine structure of acinar cells of human parotid gland. Anat. Rec. 176, 149-166.

Riva A., Motta M.P. and Riva-Testa F. (1974). Ultrastructural diversity in secretory granules of human major salivary glands. Am. J. Anat. 139, 293-298.

Riva A., Tandler B. and Testa-Riva F. (1988). Ultrastructural observations on human sublingual glands. Am. J. Anat. 181, 385-392.

Riva A., Valentino L., Lantini M.S., Floris A. and Testa-Riva F. (1993a). 3D structure of human salivary glands as seen by SEM. Microsc. Res. Tech. 26, 5-50.

Riva A., Congiu T. and Faa G. (1993b). The application of the OsO_4 maceration method to the study of human bioptic material. A procedure avoiding freze-fracture. Microsc. Res. Tech. 26, 526-527.

Simson J.A.V., Hazen D., Spicer S.S., Murphy R.A. and Young M. (1978). Secretagogue-mediated discharge of nerve growth factor from granular tubules of male mouse submandibular glands: an immunocytochemical study. Anat. Rec. 192, 375-388.

Simson J.A.V., Spicer S.S., Chao J., Grimm L. and Margolius H.S. (1979). Kallikrein localization in rodent salivary glands and kidney with the immunoglobulin-enzyme bridge technique. J. Histochem. Cytochem. 27, 1567-1576.

Spurr A. (1969). A low-viscosity epoxy resin embedding medium for electron microscopy. J. Ultrastruct. Res. 26, 31-43.

Tamarin A. and Sreebny LM. (1965). The rat submaxillary salivary gland: a correlative study by light and electron microscopy. J. Morphol. 117, 295-352.

Tanaka K. (1981). Demonstration of intracellular structures by high resolution scanning electron microscopy. In: Scanning electron microscopy. Vol. 2. Johari O. (eds). Scanning Electron Microscopy Inc. Chicago. pp 8.

Tanaka K. (1989). High resolution scanning electron microscopy of the cell. Biol. Cell 65, 89-98.

Tandler B. and Erlandson R.A. (1976). Ultrastructure of baboon parotid gland. Anat Rec. 184, 115-132.

Tandler B. and Poulsen J.H. (1976). Ultrastructure of the main excretory duct of the cat submandibular gland. J. Morphol. 149, 183-198.

Vreugdenhil A.P., de Lange G.L., Niew-Amerongen A.V. and Roukema P.A. (1980). Morphological changes in the salivary glands upon stimulation by receptor selective agonists. II. Submandibular glands of the mouse. J. Biol. Buccale 8, 73-86.

Wallace L.J. and Partlow L.M. (1976). A-adrenergic regulation of secretion of mouse saliva rich in nerve growth factor. Proc. Natl. Acad. Sci. USA. 73, 4210-4214.

Watanabe I., Ogawa K. and Yamada E. (1989). Rabbit parotid gland acini as revealed by scanning electron microscopy. Cienc. Cult. 41, 284-287.

Watanabe I., Ogawa K., Koriyama Y. and Yamada E. (1992a). Rat submandibualr gland: fractured surface observed by scanning electron microscopy. Rev. Cienc. Biomed. 13, 89-93.

Watanabe I., Koriyama Y. and Yamada E. (1992b). High resolution scanning electron microscopic study of the mouse submandibular salivary gland. Acta Anat. 143, 59-66.

Wheatly D.N. (1968). Mitochondrial tubules in the rat adrenal cortex. J. Anat. 103, 151-154.

Accepted July 14, 1995